minerals

MDPI

Article

Matese Mts. and Caserta District Karst Bauxites (Campania Region, Southern Italy): Insights on Geochemistry, Paleoclimate, Paleoenvironment, and Parental Affinity

Roberto Buccione * and Giovanni Mongelli

Department of Basic and Applied Sciences (DisBA), University of Basilicata, 85100 Potenza, Italy; giovanni.mongelli@unibas.it

* Correspondence: roberto.buccione@unibas.it

Abstract: In the Campania region (Southern Italy), in the Matese Mts. (Albian to Turonian/Coniacian) and Caserta district (Albian to Cenomanian), two karst bauxite deposits outcrop, consisting of flat lenses over shallow karst carbonate. Although the mineralogy and geochemistry of Campania bauxite deposits have been widely studied in recent years, new major and trace elements relationships were provided to highlight paleoclimatic and paleoenvironmental conditions that occurred during their formation. The purpose of this research is to provide for the first time information on the paleoclimatic and paleoenvironmental conditions that affected the bauxites of Campania. These deposits formed during different periods since the Matese deposit formed during intense weathering processes with more abundant precipitation while the Caserta district deposit experienced a more long-lasting exposure event. During the formation of the studied bauxites, the drier conditions favored the replacement of kaolinite by boehmite. R-mode factor analysis showed geochemical affinity among Al_2O_3, TiO_2, and Nb. REEs minerals are mainly associated with the bauxite matrix while Zr, Hf, and V were mainly concentrated in detrital minerals during the later stages of bauxitization. Parental affinity indices (Eu/Eu* vs. Sm/Nd; Eu/Eu* vs. TiO_2/Al_2O_3) assessed the origin of the protolith of the Campania bauxites by rejecting the hypothesis of the dissolution of the bedrock carbonate. The results confirmed the eolian transport of parental material with an Upper Continental Crust and an intermediate to mafic magmatic composition.

Keywords: karst bauxites; geochemistry; trace elements paleoclimate and paleoenvironment; Campania region

Citation: Buccione, R.; Mongelli, G. Matese Mts. and Caserta District Karst Bauxites (Campania Region, Southern Italy): Insights on Geochemistry, Paleoclimate, Paleoenvironment, and Parental Affinity. *Minerals* **2024**, *14*, 1253. https://doi.org/10.3390/min14121253

Academic Editor: Santanu Banerjee

Received: 5 November 2024
Revised: 4 December 2024
Accepted: 8 December 2024
Published: 9 December 2024

1. Introduction

Bauxites are residual rocks mainly composed of Al_2O_3 and Fe_2O_3 forming in a sub-aerial environment during tropical and subtropical climate periods and are indicators of unconformities correlated with sub-aerial carbonate exposure [1–3]. These residual rocks have been used for paleoclimatic and paleogeographic assessment [4–6]. The weathering processes which occurred during bauxite formation may favor the enrichment of several chemical elements, such as Al, Fe, and Ti, and some trace metals and the leaching of mobile elements [7,8]. To understand the processes and paleo-conditions that led to the formation of bauxites, chemical element analysis and distribution have been widely used in the last decades. These models indicate the distribution of weathering-resistant elements in bauxite deposits, such as Ti, Zr, Nb, Ta, and rare earth elements (hereafter REEs) as a tool to discover parental affinity by comparing the amounts of immobile elements in both bauxite deposits and potential parental rocks [7,9–13].

Previous studies on Italian bauxite deposits outcropping in the Apulia, Campania, Abruzzi, and Sardinia regions focused on ore deposition processes, mineralogical composition, elemental geochemistry, parental affinity, paleoclimate, and paleogeographic

restoration [5,6,8,9,12–19]. In the case of Vitulano para-autochthonous bauxites [18] major oxides such as Al_2O_3, SiO_2, Fe_2O_3, CaO, Na_2O, and K_2O were used in geochemical weathering indices that provided data on the extent of weathering conditions such as the Chemical Index of Alteration (CIA), the Chemical Index of Weathering (CIA-K), and related paleoweathering indices such as MAP^{CIA-K} and MAP-CALMAG which help to calculate the mean annual precipitation (MAP).

This paper explores the importance of the geochemistry of trace elements in the Campania karst bauxites in its two main districts which are Matese and Casertano, Southern Apennines. Several trace elements and their ratios, such as Sr/Cu and Sm/Nd have been used to retrieve information related to paleoclimate and paleoenvironmental conditions and on the parent rock that led to the formation of the studied bauxites.

2. Geological Framework

Campania karst bauxites outcrop in the Southern Apennines (Figure 1) which are defined by the tectonic superposition of several thrust sheets consisting of Meso-Cenozoic deep basin to shallow-water succession.

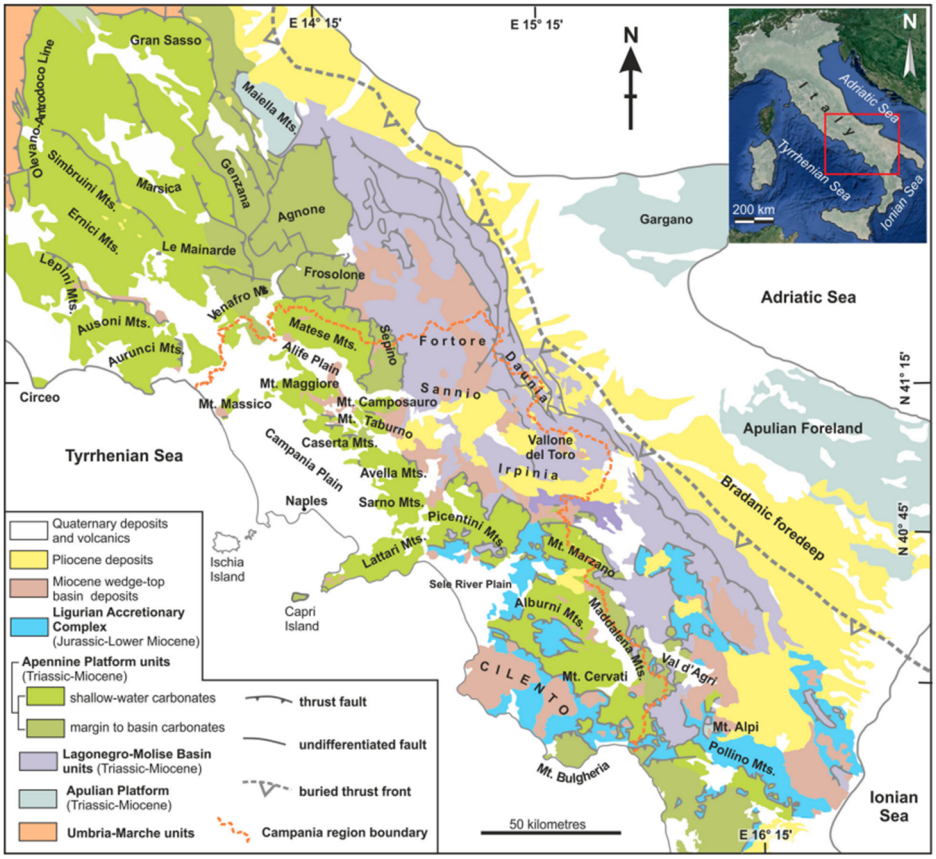

Figure 1. Geological map of Southern Apennines from Vitale and Ciarcia [20].

The formation of bauxite requires events of sub-aerial carbonate exposure. Although Italian bauxites have a well-defined stratigraphic framework, the processes that favored the carbonate platform sub-aerial exposure, promoting their formation, have remained debated for a long time. In the Campania region, karst bauxite deposits are associated with a thick Meso-Cenozoic carbonate succession, building the main portion of the Matese and the Mt. Maggiore Mountain chains (Figure 2) [21]. These carbonate successions are the product of the deformation of a paleogeographic scenario which was characterized, from the Triassic to the Early Miocene, by carbonate sedimentation, interspersed with several stratigraphic gaps. These carbonate successions correspond to the Apennine carbonate platform [21].

The Apennine fold-and-thrust Belt evolved from the Late Cretaceous, through a convergent movement between the African and European plates [22]. The Mesozoic sediments include a platform-dominated succession, deeper basal successions, and the Apennine carbonate platform [23]. The Apennine carbonate platform was placed at tropical latitudes, around 20° N, between the Panormide carbonate platform and the Apulian carbonate platform [24]. During the Late Aptian-Cononian, the Apennine platform experienced repeated and long-lasting emersions, evidenced by bauxites; the duration of these emersion events was variable [2].

During the Middle Cretaceous, these stratigraphic gaps were temporally variable, which supports the hypothesis of a complex paleo-topography controlled by tectonic events [25]. D'Argenio and Mindszenty [2] hypothesized that a lithospheric bulge, caused by the early phases of the orogenic collision, was responsible for the long-duration exposure of some sectors of the Southern Apennine platform during the Cretaceous. More recent work [24] proposes the existence of an E-W lateral slip fault which induced the rise and the exposure of the carbonate platforms. In any case, the carbonate exposures resulted in extensive karstification and, in general, the deposition of bauxite deposits [25,26].

From the Upper Cenomanian to the Coniacian, the bauxite deposits are unconformably covered by carbonate sediments dated from the Upper Cenomanian to the Coniacian. The limestone below the unconformity is significantly karstified and preserves a complex diagenetic record consisting of events such as dissolution, cementation, and internal sedimentation [27]. In the eastern portion of the Matese Mountains (Regia Piana and Bocca della Selva) the stratigraphic gap ranges from the Middle-Upper Albian to the Turonian-Lower Coniacian [21]. In the Caserta district, the stratigraphic gap is more limited covering the Albian-Cenomanian transition [25].

The Campania bauxite deposits (Matese Mts. and Caserta district) consist of flat lenses (a few meters thick) above shallow karst carbonate. Only in the Mt. Maggiore bauxites, in the Caserta district, the thickness of the flat bauxite layer suddenly increases, reaching a depth of about 10 m, at the Castello di Dragoni mining site [27].

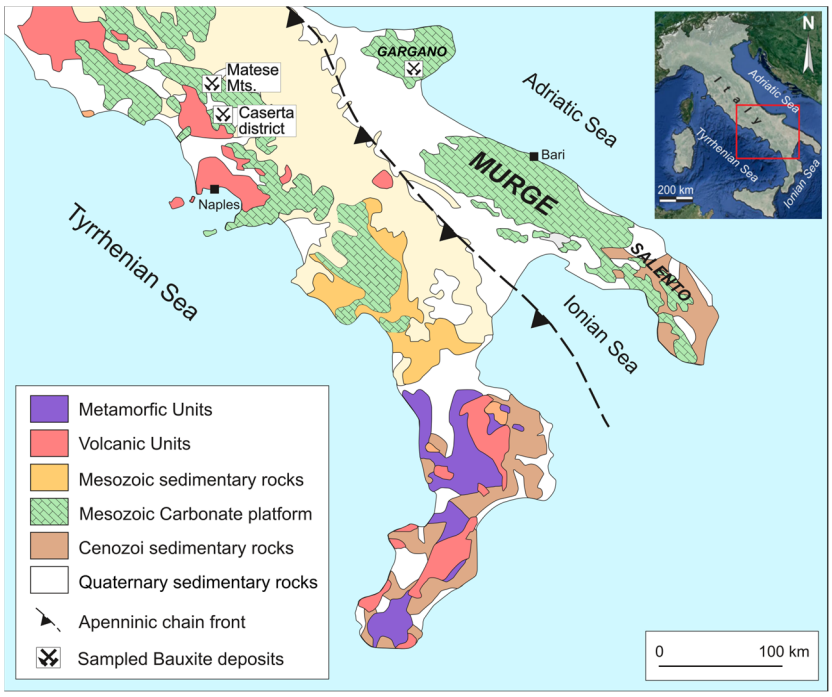

Figure 2. Geo-lithological map of the Southern Apennines. In red square the studied area. The studied deposits are shown. Modified after Bonardi et al. [28].

3. Sampling and Analytical Techniques

Of the eighteen bauxite samples collected from the Matese Mts. (Bocca della Selva and Regia Piana), six samples have never been analyzed, while the remaining samples are from Mondillo et al. [15]. Regarding the thirteen new samples which were studied from the Matese Mts. and the Caserta district, seven new samples were taken from the Dragoni quarry (DR1-DR7) while six new samples were taken from the Matese Mts. (MA1-MA6); the rest of the samples are from Mondillo et al. [15].

Geochemical analysis of the studied samples was performed at ACME Analytical Laboratories Ltd. (Vancouver, BC, Canada). The samples were pulverized to 85%—200 mesh, to obtain about 20 g of pulp. Major oxides and several trace elements were analyzed by using ICP-OES following a $LiBO_2/Li_2B_4O_7$ fusion and dilute nitric digestion. Rare earth elements were determined by ICP-MS following a $LiBO_2/Li_2B_4O_7$ fusion and nitric acid digestion. Loss on ignition (LOI) derives from weight difference after ignition at 1000 °C [18].

Semi-quantitative mineralogical analysis was performed by X-ray powder diffraction (XRPD) at the Institute of Earth Sciences, Heidelberg University (Heidelberg, Germany) with a Siemens D 500 Bragg-Brentano X-ray diffractometer, with CuKα radiation, 40 kV and 30 mA, 5 s/step and a step scan of 0.05° 2θ while SEM analysis was performed using a Jeol JSM 5310 instrument at the University of Napoli (Napoli, Italy) (CISAG).

4. Results

4.1. Mineralogy and Micromorphology

The texture of Campania bauxites is mainly oolitic to pisolitic with the occurrence of Al(-Fe) hydroxides dispersed in a clay matrix (Figure 3a). The structure of the ooids is often composed of alternating concretions of different mineralogical compositions, generally consisting of boehmite, goethite, and hematite (Figure 3b). In fact, boehmite, hematite, and goethite are more abundant in the ooid structure, whereas kaolinite is mostly enriched in the bauxite matrix (Figure 3c). Generally, the cores of the ooids consist of older, detrital bauxite pebbles, or hematite-goethite or boehmite fragments (Figure 3d).

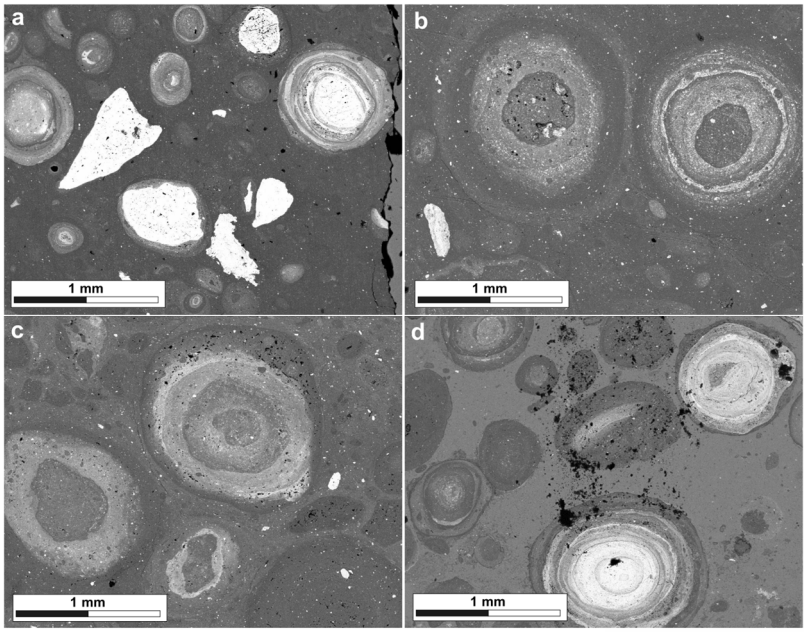

Figure 3. SEM images of studied Campania bauxites. (**a**) Texture of Campania bauxites with occurrence of Al(-Fe) hydroxides dispersed in a clay matrix; (**b**) photo of the bauxites texture composed of alternating concretions of different mineralogical composition; (**c**) bauxite texture with several large ooids in a clayey matrix; (**d**) ooids formed by cores of detrital bauxite pebbles, or hematite-goethite fragments.

The mineral composition of the studied bauxites is quite similar and is generally dominated by boehmite which is the main Al-rich mineral, exhibiting abundances of 50.0–75.0 wt.% (Figure 4). The silica-bearing phases are mostly clay minerals, and the most abundant phase is kaolinite ranging from 3 to 20 wt.%. In the Caserta district deposit, traces of illite/smectite also occur while gibbsite has been identified only in some samples such as GRBX 3 and BXDRA 6. Hematite is the main Fe-bearing mineral, with an average of 15.0 wt.% in both bauxite districts. Anatase has been identified in both bauxite deposits showing an average between 7 and 10.0 wt.%. Finally, traces of zircon and monazite were found in some samples of Caserta district bauxites.

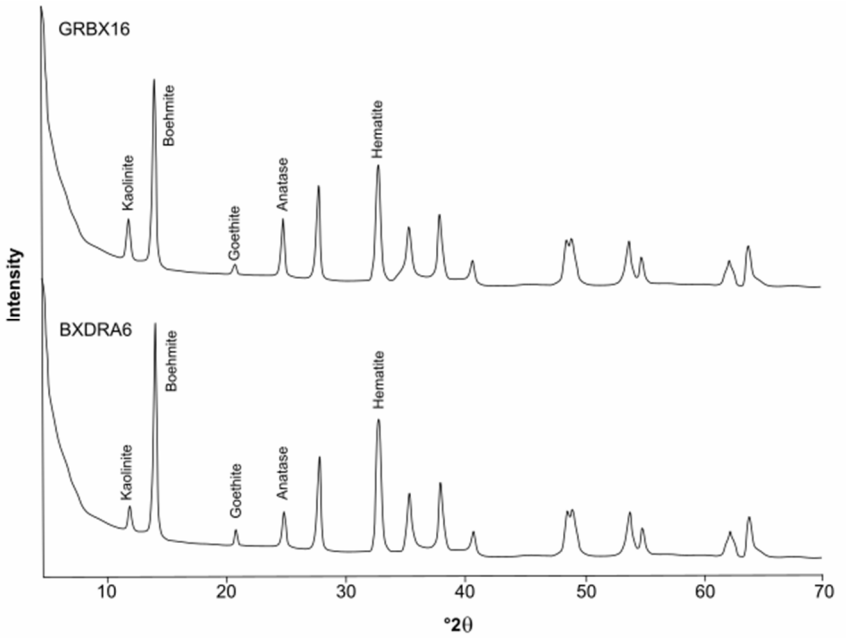

Figure 4. XRD patterns of two selected representative samples of Matese Mts. and Caserta district bauxites.

4.2. Geochemistry of Major and Trace Elements

The chemical composition of the studied bauxite deposit is listed in Table 1. The most abundant major oxides are Al_2O_3 (Matese Mts. median = 59.1 wt.%; Caserta district median = 50.0 wt.%), Fe_2O_3 (Matese Mts. median = 14.6 wt.%; Caserta district median = 30.0 wt.%), and SiO_2 (Matese Mts. median = 6.7 wt.%; Caserta district median = 3.6 wt.%) (Figure 5).

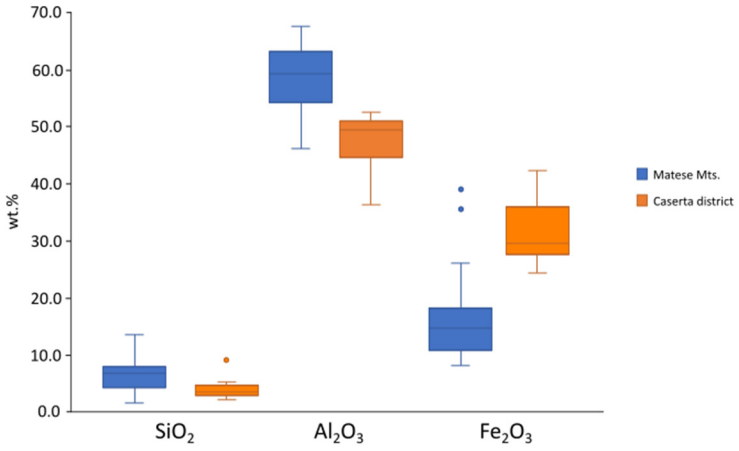

Figure 5. Box and whiskers plot of major oxides (wt.%) in the Matese and Caserta district bauxites. Blu and orange dots indicate the upper and lower outliers.

Table 1. Major (%) and trace elements (ppm) compositions of Campania bauxites. Geochemical data are from [15]. Geochemical data from MA1 to MA6 and from DR1 to DR7 are data from this work.

Samples	SiO_2	Al_2O_3	Fe_2O_3	TiO_2	CaO	Na_2O	K_2O	MgO	Cr	Ni	Zr	V	Co	Ba	Cu	Th	U	Sc	Sr	Ga	Hf
Matese Mts.																					
GRBX3	11.2	52.6	14.7	2.4	0.1	0.05	0.17	0.22	500	243	478	293	37.8	42	12.8	100.1	26.1	-	273.7	-	15.8
GRBX4	6.9	63.0	10.0	3.1	0.2	0.04	0.15	0.22	600	163	524	294	19.3	39	9.3	57.8	18.7	-	39.8	-	16.4
GRBX7	7.2	62.2	10.8	2.8	0.1	0.04	0.10	0.20	600	174	499	328	22.4	30	10.9	60.0	6.1	-	249.6	-	15.6
GRBX8	7.3	58.6	17.4	3.0	0.1	0.04	0.11	0.19	600	174	571	440	23.1	21	8.9	87.2	7.8	-	79.5	-	18.5
GRBX9	6.5	63.0	11.6	3.3	0.1	0.03	0.11	0.22	700	154	596	421	21.8	17	10.3	83.0	5.9	-	76.6	-	19.3
GRBX12	8.1	50.5	26.0	2.5	0.2	0.05	0.12	0.20	500	159	519	462	22.3	24	11.4	86.6	11.4	-	59.1	-	16.3
GRBX13	11.0	54.7	14.7	2.7	0.3	0.05	0.16	0.20	600	246	535	321	39.6	47	13.9	113.0	26.4	-	328.1	-	17.1
GRBX14	3.8	67.5	10.5	3.4	0.1	0.02	0.05	0.13	600	82	546	346	18.2	15	7.9	58.8	8.2	-	77.3	-	18.4
GRBX15	3.7	62.5	16.9	3.1	0.1	0.03	0.04	0.11	600	93	505	398	19.2	17	6.2	41.6	12.8	-	84.2	-	16.5
GRBX16	4.4	64.3	14.3	3.1	0.1	0.02	0.05	0.13	600	103	524	352	26.6	14	12.0	46.7	11.5	-	82.5	-	15.9
GRBX17	1.5	46.0	39.0	2.5	0.1	0.01	0.01	0.06	800	126	494	342	33.3	28	55.6	68.5	5.1	-	32.9	-	16.5
GRBX18	1.7	48.6	35.4	2.6	0.1	0.03	0.01	0.07	700	132	488	282	31.8	31	54.7	53.6	4.5	-	35.6	-	14.3
MA1	13.5	59.5	8.3	3.0	0.1	0.08	0.11	0.18	410	80	500	244	24.0	43	9.0	37.3	7.8	40.0	474.0	53.0	14.0
MA2	7.0	55.1	17.2	2.8	0.8	0.05	0.08	0.16	470	150	503	729	24.0	48	20.0	55.6	8.7	61.0	841.0	61.0	14.1
MA3	4.7	58.8	14.4	2.9	1.3	0.04	0.06	0.16	430	140	516	514	21.0	56	20.0	59.1	7.7	71.0	1161.0	62.0	13.8
MA4	5.1	62.9	11.0	3.0	0.4	0.04	0.07	0.17	440	150	529	383	22.0	64	20.0	51.3	7.3	56.0	1108.0	65.0	14.6
MA5	5.6	58.2	19.8	2.8	0.1	0.04	0.07	0.16	350	160	553	347	17.0	20	10.0	76.5	9.5	74.0	61.0	48.0	14.5
MA6	7.9	63.8	8.0	2.8	0.1	0.04	0.11	0.19	380	170	535	266	19.0	34	20.0	54.0	4.8	76.0	202.0	59.0	14.6
Caserta dst.																					
BXRA1	9.1	36.8	38.0	2.0	0.3	0.04	0.37	0.28	600	143	385.2	732.0	32.7	47	81.1	35.3	18.4	-	-	-	11.4
BXDRA4	5.1	51.1	28.7	2.5	0.2	0.03	0.07	0.14	700	225	432.9	244.0	37.2	26	72.0	46.3	5.4	-	-	-	12.0
BXDRA5	2.2	48.8	33.2	2.4	0.9	0.03	0.02	0.15	700	158	462.6	288.0	40.8	33	45.6	58.2	5.4	-	-	-	13.5
BXDRA6	3.3	53.2	24.7	2.6	0.2	0.05	0.09	0.21	800	253	449.9	406.0	118.6	26	332.9	51.9	16.4	-	-	-	12.7
BXMAI8	3.6	42.6	40.8	2.2	0.1	0.03	0.07	0.13	900	416	428.4	465.0	50.8	33	69.2	64.3	5.6	-	-	-	13.6
BXDRA9	4.5	50.0	30.0	2.4	0.1	0.03	0.15	0.25	700	354	441.4	341.0	46.4	30	83.2	50.4	5.6	-	-	-	12.0
DR1	5.2	51.6	25.9	2.4	0.2	0.03	0.04	0.24	440	200	454.0	256.0	35.0	35	50.0	41.3	6.3	61.0	49.0	50.0	11.7
DR2	3.3	52.2	27.4	2.6	0.2	0.04	0.02	0.16	500	110	522.0	265.0	44.0	28	60.0	48.0	5.9	65.0	27.0	61.0	14.1
DR3	2.5	51.3	29.5	2.5	0.2	0.04	0.03	0.18	420	200	532.0	287.0	67.0	37	70.0	50.9	6.0	71.0	27.0	50.0	13.9
DR4	2.7	51.5	28.9	2.6	0.2	0.04	0.04	0.17	410	200	533.0	271.0	39.0	32	60.0	48.4	5.9	68.0	28.0	49.0	13.7
DR5	3.6	38.5	42.7	2.2	0.3	0.04	0.02	0.24	450	250	505.0	369.0	51.0	52	60.0	65.7	7.3	89.0	23.0	47.0	13.5
DR6	3.7	48.3	31.1	2.6	0.2	0.03	0.03	0.21	420	200	507.0	291.0	37.0	38	50.0	51.8	5.4	72.0	28.0	48.0	11.4
DR7	3.1	47.8	34.6	2.5	0.2	0.02	0.02	0.18	450	220	528.0	313.0	42.0	38	60.0	55.6	5.7	76.0	26.0	48.0	13.7

Table 1. *Cont.*

Samples	Nb	Y	La	Ce	Pr	Nd	Sm	Eu	Gd	Tb	Dy	Ho	Er	Tm	Yb	Lu	∑REE	Ce/Ce*	Eu/Eu*	$(La/Yb)_{cho}$	Sr/Cu
GRBX3	49.0	48.3	308.5	712.6	51.7	155.2	16.9	3.1	14.4	2.0	10.1	2.0	6.2	1.1	7.2	1.1	1340.4	1.3	0.6	28.9	28.9
GRBX4	62.0	57.1	67.1	131.6	16.4	62.1	11.4	2.4	10.4	1.9	10.7	2.2	6.8	1.2	8.2	1.3	390.8	0.9	0.6	5.5	5.5
GRBX7	54.2	57.6	79.9	155.0	18.5	69.1	12.9	2.6	11.2	1.9	11.1	2.3	7.1	1.2	7.8	1.3	439.5	0.9	0.6	6.9	6.9
GRBX8	56.2	64.0	87.7	154.1	19.8	74.2	13.4	2.9	12.0	2.1	11.9	2.5	7.7	1.3	8.4	1.3	463.3	0.8	0.7	7.0	7.0
GRBX9	65.1	62.3	66.7	220.7	17.9	67.4	12.8	2.6	11.6	1.9	11.4	2.3	7.1	1.2	7.9	1.2	495.0	1.5	0.6	5.7	5.7
GRBX12	48.7	78.8	108.7	693.1	32.8	129.1	27.0	5.9	27.1	4.0	20.6	3.8	10.3	1.7	10.9	1.7	1155.5	2.7	0.6	6.7	6.7
GRBX13	56.0	52.1	354.7	828.1	55.3	151.0	15.7	2.7	14.6	2.0	11.3	2.2	6.6	1.1	7.8	1.2	1506.4	1.3	0.5	30.7	30.7
GRBX14	65.2	54.6	45.1	104.8	11.0	42.7	7.9	1.7	7.9	1.5	9.4	2.1	6.1	1.1	7.0	1.1	304.0	1.1	0.6	4.3	4.3
GRBX15	60.2	51.8	52.1	115.1	13.5	51.3	10.4	2.2	9.4	1.7	9.8	2.1	6.3	1.1	7.3	1.1	335.2	1.0	0.6	4.8	4.8
GRBX16	61.5	50.2	45.3	90.6	11.0	46.0	8.5	1.8	8.2	1.5	9.3	1.9	5.9	1.0	6.6	1.0	288.8	0.9	0.6	4.6	4.6
GRBX17	47.5	58.8	107.2	232.4	24.6	89.0	16.6	3.5	13.7	2.3	12.9	2.4	6.9	1.2	7.5	1.1	580.1	1.0	0.7	9.6	9.6
GRBX18	49.2	61.0	106.0	278.3	24.1	92.4	16.9	3.6	14.6	2.4	13.0	2.6	7.9	1.3	7.9	1.2	633.2	1.2	0.7	9.0	9.0
MA1	61.0	40.0	62.0	126.0	12.0	45.2	8.4	1.5	6.0	1.1	7.3	1.6	5.2	0.8	5.7	0.9	323.7	1.0	0.6	7.3	7.3
MA2	57.0	45.0	74.3	127.0	12.6	46.5	9.7	2.0	8.3	1.5	9.7	2.0	6.1	0.9	6.6	1.1	353.3	0.9	0.6	7.6	7.6
MA3	57.0	47.0	88.8	142.0	14.1	49.7	10.5	2.1	8.8	1.6	9.7	1.9	6.2	1.0	6.7	1.1	391.2	0.9	0.6	8.9	8.9
MA4	61.0	48.0	80.2	124.0	13.5	52.4	11.1	2.3	8.6	1.5	10.1	2.2	6.5	1.0	7.5	1.2	370.1	0.8	0.7	7.2	7.2
MA5	54.0	52.0	72.2	140.0	16.9	63.5	12.5	2.7	10.0	1.8	11.7	2.4	7.1	1.1	8.0	1.3	403.2	0.9	0.7	6.1	6.1
MA6	58.0	51.0	45.9	78.8	10.4	40.5	9.5	2.0	8.4	1.7	10.7	2.3	7.2	1.1	7.8	1.3	278.6	0.8	0.6	3.9	3.9
BXRA1	36.1	51.5	102.0	231.4	27.2	101.8	17.7	3.6	14.5	2.1	10.8	1.9	5.3	0.8	5.4	0.8	576.8	1.0	0.6	12.7	12.7
BXDRA4	43.7	75.8	114.0	230.9	28.4	106.7	19.8	4.2	17.3	2.9	16.4	3.3	9.7	1.4	9.1	1.4	641.3	0.9	0.6	8.4	8.4
BXDRA5	47.0	73.4	129.3	325.4	31.5	117.2	21.0	4.4	17.5	2.8	15.3	3.1	9.1	1.3	8.6	1.3	761.2	1.1	0.7	10.1	10.1
BXDRA6	47.8	67.7	135.2	392.8	39.1	149.7	27.9	5.6	21.8	2.9	13.7	2.5	7.3	1.1	7.4	1.2	875.9	1.2	0.6	12.3	12.3
BXMAI8	39.8	67.3	146.7	320.5	33.3	126.4	22.6	4.7	18.9	2.9	15.9	3.0	9.1	1.4	8.8	1.4	782.9	1.0	0.6	11.2	11.2
BXDRA9	45.3	108.8	125.9	233.8	29.6	109.5	20.8	4.6	21.2	3.3	19.0	3.8	10.9	1.5	9.8	1.5	704.0	0.9	0.6	8.6	8.6
DR1	48.0	61.0	130.0	260.0	29.6	111.0	20.7	4.2	15.5	2.3	13.9	2.7	7.6	1.2	8.0	1.2	669.0	0.9	0.7	10.9	10.9
DR2	54.0	68.0	135.0	309.0	31.5	118.0	22.5	4.6	16.3	2.7	16.3	3.2	9.3	1.4	9.1	1.5	748.3	1.1	0.7	10.0	10.0
DR3	54.0	67.0	131.0	409.0	32.4	125.0	24.4	4.9	17.3	2.7	15.9	3.1	9.1	1.4	9.1	1.4	853.7	1.4	0.7	9.7	9.7
DR4	52.0	66.0	126.0	353.0	31.6	119.0	23.2	4.6	16.1	2.6	15.6	2.9	8.7	1.3	8.8	1.4	780.8	1.3	0.7	9.6	9.6
DR5	46.0	70.0	168.0	408.0	41.2	159.0	29.5	6.1	20.7	3.4	18.8	3.6	10.1	1.4	9.1	1.4	950.3	1.1	0.7	12.4	12.4
DR6	37.0	68.0	140.0	335.0	34.1	127.0	24.5	5.1	17.1	2.8	15.7	3.2	8.9	1.3	8.8	1.4	792.8	1.1	0.7	10.7	10.7
DR7	53.0	66.0	132.0	283.0	29.9	113.0	21.4	4.5	15.8	2.7	15.8	3.1	9.0	1.3	8.9	1.4	707.8	1.0	0.7	10.0	10.0

The classification diagrams [29–31] of the Campania region karst bauxites show some differences in the amount of Al_2O_3, which is higher in the Matese Mts. bauxites, while Fe_2O_3 is higher in the bauxites of the Caserta district. The geochemical classification of bauxites places most of the bauxites from the Caserta district in the field of "ferritic bauxites" while the bauxite samples of the Matese Mts. deposit fall within the field of "ferritic bauxites" and "bauxites" since they display higher Al_2O_3 values (Figure 6).

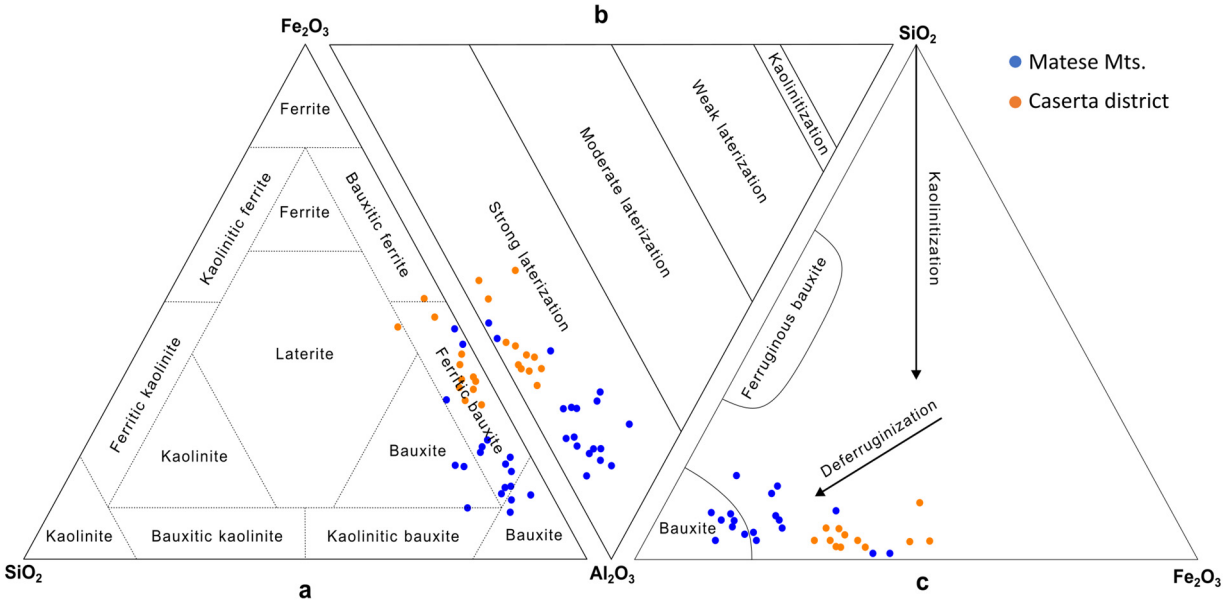

Figure 6. Ternary classification diagrams for Campania region bauxites [29–31]. (**a**) Bauxite classification after [29]; (**b**) Laterization degree diagram after [30]; (**c**) Bauxite classification with deferrugination degree after [31].

Regarding the degree of lateralization, all the bauxite samples (both Matese and Caserta districts) fall within the field of "strong laterization" and finally, it was observed that the bauxites from the Matese recorded a higher deferrification degree with respect to the bauxites from the Caserta district, which, as observed in the results section, are naturally more enriched in Fe_2O_3. Regarding trace elements, the most abundant are Cr (Matese Mts. median = 600 ppm; Caserta district median = 500 ppm), Ni (Matese Mts. median = 152 ppm; Caserta district median = 200 ppm), Zr (Matese Mts. Median = 521.5 ppm; Caserta district median = 462.6 ppm), and V (Matese Mts. median = 346.5 ppm; Caserta district median = 291 ppm). Further trace elements show amounts such as Co (Matese Mts. median = 22.4 ppm; Caserta district median = 42 ppm), Ba (Matese Mts. median = 30.5 ppm; Caserta district median = 33.0 ppm), Cu (Matese Mts. median = 11.7 ppm; Caserta district median = 60 ppm), Th (Matese Mts. median = 59 ppm; Caserta district median = 50.9 ppm), U (Matese Mts. median = 8 ppm; Caserta district median = 50.9 ppm), Sc (Matese Mts. median = 66 ppm; Caserta district median = 71 ppm), Sr (Matese Mts. median = 83.4 ppm; Caserta district median = 27 ppm), Ga (Matese Mts. median = 60 ppm; Caserta district median = 49 ppm), Hf (Matese Mts. median = 15.9 ppm; Caserta district median = 13.5 ppm), Nb (Matese Mts. median = 57 ppm; Caserta district median = 47 ppm), and Y (Matese Mts. median = 52.1 ppm; Caserta district median = 67.7 ppm) were also observed. The most enriched chemical elements of the REE group are La (Matese Mts. median = 77.1 ppm; Caserta district median = 131 ppm) and Ce (Matese Mts. median = 141 ppm; Caserta district median = 320.5 ppm). The total ∑REE is more abundant in the Caserta district bauxites (median = 761.2 ppm) with respect to Matese Mts. bauxites (median = 397.2 ppm). Three samples of Matese bauxites show the highest ∑REE values (GRBX3 = 1340.4 ppm; GRBX12 = 1155.5 ppm; GRBX13 = 1506.4 ppm). The chondrite-normalized REE patterns (chondrite values are from Taylor and McLennan, 1985) show a general moderate fraction-

ation with $(La/Yb)_{cho}$, median values of 7 and 10 for Matese Mts. and Caserta district bauxites, respectively (Figure 7).

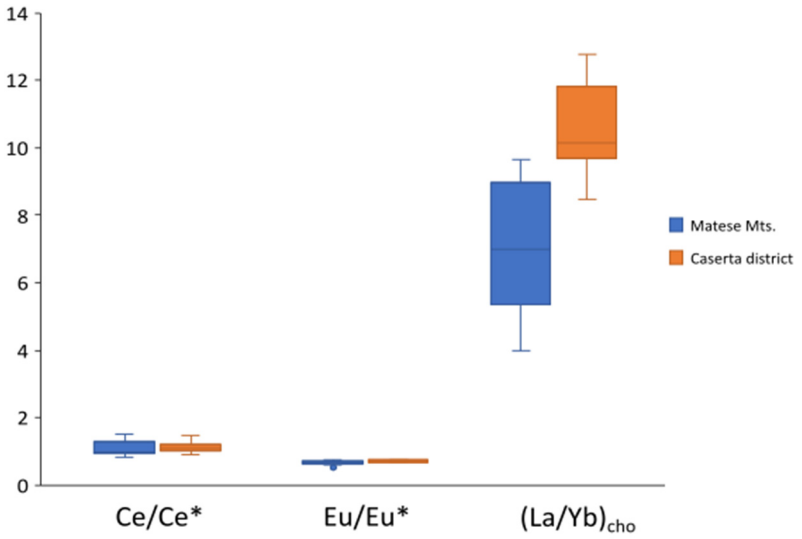

Figure 7. Box and whiskers plot of Ce anomaly, Eu anomaly, and $(La/Yb)_{cho}$ fractionation index in the Matese and Caserta district bauxites.

Only two samples (GRBX 3 and GRBX 13) display slightly higher fractionation with $(La/Yb)_{cho}$ values of 28.95 and 30.73, respectively. The Ce anomaly values in the Campania deposits tend to remain close to unity with the exception of one sample of the Matese Mts. bauxite deposit that has a value greater than two (GRBX12 = Ce/Ce* 2.72). The Eu/Eu* in the Campania bauxite deposits shows a very conservative trend and very low variability (Matese Mts. bauxites Eu/Eu* median = 0.70; Caserta district bauxites Eu/Eu* median = 0.74) (Figure 8).

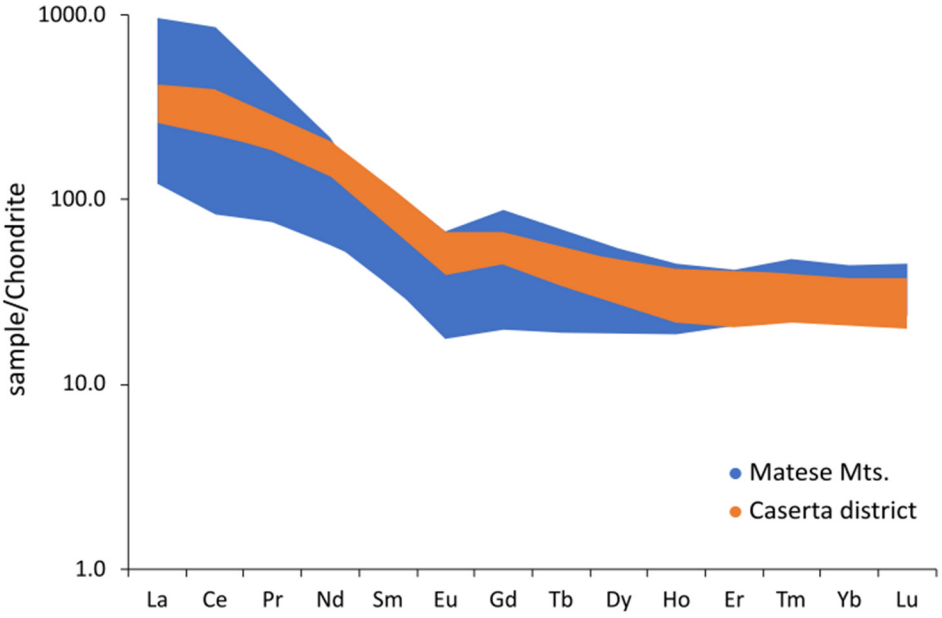

Figure 8. Chondrite-normalized REEs patterns of Matese and Caserta district bauxite samples. Chondrite values are from Taylor and McLennan [32].

5. Discussion

5.1. Factors Controlling Element Distribution

An R-mode factor analysis, including major oxides Al_2O_3, Fe_2O_3, SiO_2, and TiO_2 and several trace elements such as Ni, Zr, V, Hf, Nb, Y, and ∑REEs, was performed to evaluate inter-elemental relationships. Factors were extracted after Varimax rotation using the STATGRAPHICS Centurion XVI.I version package, software using a standardized correlation matrix, thereby weighting all the variables equally during factor calculations. The commonalities provide an index of the efficiency of the proposed set of factors [33], and the magnitude of the commonalities calculated in this study suggests that most of the original variance is still accounted for by the present set of factors.

Factor Analysis of Campania region bauxites provided three factors which explain 81.40% of the total variance in the geochemical database (Table 2). The first factor (F1; Var.% = 48.19) shows highly positive weightings for Al_2O_3, TiO_2, and Nb and negative weightings for Fe_2O_3, Ni, Y, and total REE. Al_2O_3 and TiO_2 are concentrated during the formation of bauxite in Al-hydroxides and Ti-oxide. Nb, which shares similar geochemical behavior with Ti, may also be hosted in the mineral anatase (TiO_2). In karst bauxites, these elements are usually covary and their distribution is generally promoted by dry climate conditions [6]. As for Ni, in karst bauxites, its mobility is often controlled by Fe-oxyhydroxides [34] as well as it may occur, to some extent, for the REE + Y pool [9]. Since during bauxitization the iron-rich oxyhydroxide accumulation is favored by wet conditions, F1 likely accounts for the competition of elements whose concentration is mostly driven by different climate regimes [5]. The second factor (F2; Var.% = 22.77) shows positive weightings for Hf, Zr, and V which are elements characterized by low solubility during intense weathering conditions. F2 thus accounts for the capability of minerals of the resistate pool such as zircon (Hf-Zr) and Ti-oxide to accumulate during bauxitization. The third factor (F3; Var.% = 10.43) includes only positive weighting for SiO_2. It is well known that the main silica-bearing mineral in Campania bauxites, and in general in all Southern Italy bauxites, is mainly kaolinite that, in our case, is confined to the matrix as a secondary mineral due to local re-silicification of boehmite [15]. Therefore, F3 likely describes the process of re-silicification during the bauxite formation related to the replacement of boehmite by the main silica-bearing minerals.

Table 2. R-mode Factor Analysis results for Campania region bauxite deposits.

	Factor 1	Factor 2	Factor 3
SiO_2			0.91
Al_2O_3	0.90		
Fe_2O_3	−0.80		
TiO_2	0.87		
Ni	−0.80		
Zr		0.74	
V		0.80	
Hf		0.76	
Nb	0.82		
Y	−0.69		
∑REE	−0.80		
Var.%	48.19	22.77	10.43

Note: Numbers are weights of the variables in the extracted factors. Variables having a weight of less than 0.70 are omitted.

5.2. Paleoweathering and Paleoclimate

Climatic conditions have an extreme influence on sediment geochemistry due to their control over the weathering process [35–37]. However, intense weathering is associated with a warm and humid climate, while less intense and less aggressive weathering processes are associated with a cold and arid climate [37]. According to Suttner and Dutta [38], this interpretation is confirmed by the SiO_2 versus (Al_2O_3 + K_2O + Na_2O) binary diagram,

where the bauxites from Campania all fall within the arid climate range. It must be noted that by observing (Figure 9) it can be stated that bauxites from Matese Mts. fall in a "more arid" field with respect to Caserta district bauxites which fall close to the "semi-arid" field.

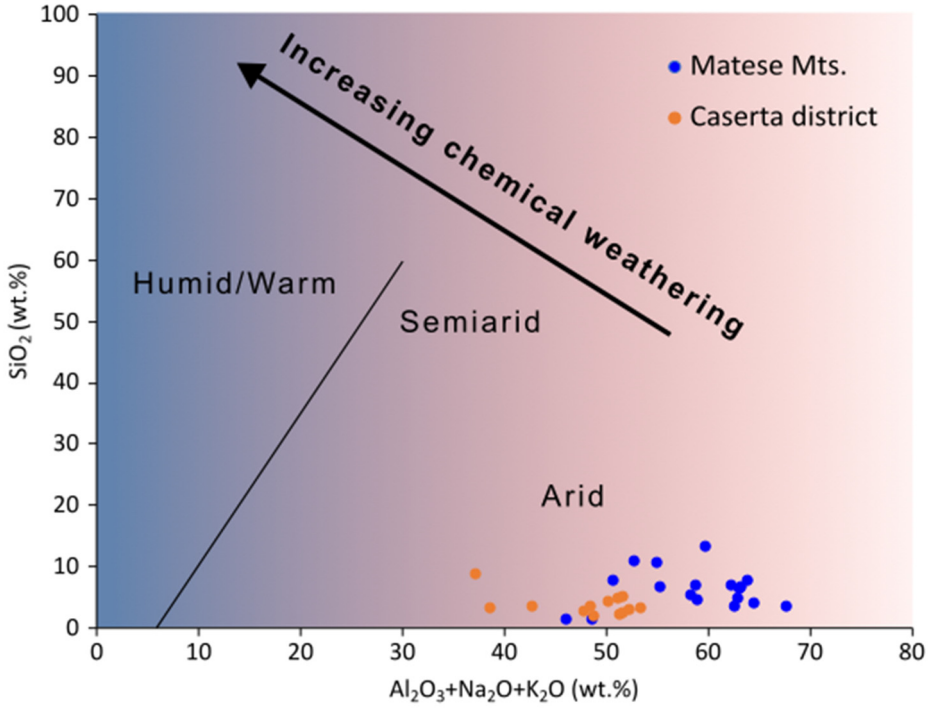

Figure 9. SiO_2 vs. (Al_2O_3 + K_2O + Na_2O) binary diagram from Suttner and Dutta [38]. The background color in the figures indicate the increasing chemical weathering moving from light red to blue.

Some trace elements, such as Sr and Cu, which are useful indicators of paleoclimatic conditions, can be used to assess paleoclimatic conditions [39,40] and it is suggested that Sr/Cu ratios above 5.0 reflect a warm-arid climate, while a low Sr/Cu ratio in the range of 1.3–5.0 indicates a warm-humid climate [39]. The bauxites in Campania have quite different values, suggesting that the bauxites in the Matese Mts., which have a median of 9.94, were formed in a more arid and aggressive climate in a more humid climate than the bauxites in the Caserta district, which have lower values of the Sr/Cu ratio (median = 0.45) and are therefore associated with a warmer climate and less aggressive climate conditions.

The relationship between mobile and immobile elements has been widely used to reconstruct the weathering conditions affecting the source area, and one of the most used weathering indices for assessing the paleoclimate and paleoweathering conditions in residual sediments is the Chemical Index of Alteration (CIA) [41–43].

The CIA was calculated using the formula: CIA = [Al_2O_3/(Al_2O_3 + CaO* + Na_2O + K_2O)] × 100, where CaO* is the amount of CaO only regarding silicate phases [44]. Of course, bauxites, which are highly weathered residual rocks, generally have CIA values higher than 90%. Accordingly, the CIA values of studied bauxites are very high since the median is 99.78% in Matese Mts. bauxites and 99.92% in the Caserta district bauxites. The results of weathering indices show that the degree of weathering is very high, and this is a typical characteristic of bauxites that form under high weathering conditions.

The chemical composition of paleo-soils is an interesting tool to assess paleoprecipitation [44] by using the climo-functions CIA-K (100 × (Al/(Al + Ca + Na))) [45] and CALMAG (100 × (Al/(Al + Ca + Mg))) [46]. These climo-functions can give information about the related mean annual precipitation $MAP^{CIA\text{-}K}$ (mm/y) = $221.1^{e0.0197(CIA\text{-}K)}$ [42] and MAP-CALMAG (mm/y) = 22.69 (CALMAG) − 435.8.

In the Matese Mts. bauxites, CIA-K values have a median of 99.73% while in the Caserta district, the median is 99.56%. CALMAG shows a median of 99.49% in the Matese

Mts. bauxites whereas in the Caserta district, the median is 99.23%. The mean annual precipitation MAP-CALMAG in Matese Mts. has a median of 1821.6 mm/year while in the Caserta district is 1815.8 mm/year while the values of MAP^{CIA-K} showed that in the Matese Mts. the median is 1576.9 mm/year and in the Caserta district the median value is 1569.8 mm/year (Figure 10). The paleoprecipitation values (MAP—CALMAG and MAP^{CIA-K}) of the two Campania bauxite deposits are quite similar but slightly higher values are observed for some samples of the Matese bauxites, and this is in accordance with the more "humid" conditions which affected Matese Mts. deposits with respect to Caserta district bauxites.

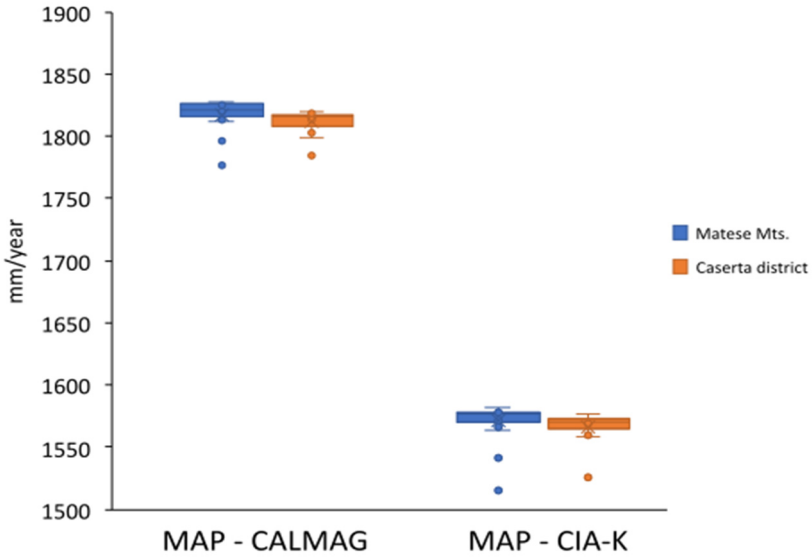

Figure 10. Box and whiskers plot of CIA-K and CALMAG climo-functions in the Matese and Caserta district bauxites. Orange and blue dots indicate the outliers.

5.3. Parental Affinity

Numerous attempts have been made to identify bauxite source rock and the processes that lead to their formation. However, the karst bauxite source rock provenance is still largely debated. It has been demonstrated that the origin of karst bauxites is not related to the dissolution of carbonate bedrock [5,6,9,15]. A wide range of different lithologies has suggested protoliths for karstic bauxites, including river-borne debris from basement rocks [1], windblown material [47,48], clayey components of underlying limestone [49,50], ancient mafic basement material, windblown volcanic ash [1,51–53], and a mixed source of limestone and andesite basement [6,9].

The formation process of karst bauxite is generally accompanied by significant fractionation of major, trace, and rare earth elements. For this reason, it is not easy to recognize the relative contributions of the various sources [54] and the assessment of parental relationships [5,9] during bauxite formation, especially in a period such as the Mesozoic, and in a region such as the Tethys, a scenario characterized by strong tectonic activity [24]. Al_2O_3 and TiO_2, due to their high water/crust partition coefficients and very low residence times [31], have significant potential to be transferred into sedimentary rocks, preserving valuable information about the parent rock. Trace elements such as Sm and Nd are widely used to assess bauxite parental affinity since they show only minor fractionation during intense tropical weathering [9].

The Eu anomaly acts as a conservative index during bauxitization [50] and remains almost unchanged during intense weathering processes [9]. The Eu/Eu* ratio is also an index of chemical differentiation [9] and preserves the value of the original rock more than other source indices [55,56], even during bauxite development [15].

The TiO_2/Al_2O_3 relationship is largely used to trace the parent rock of bauxites because this ratio is a sensitive index of parental affinity and records the content of the

protolith when both elements behave conservatively [9,16]. Several methods have been used, including the relationship between immobile elements diagrams [50,57].

Parental affinity diagrams (Figures 11 and 12), using Eu/Eu* vs. TiO_2/Al_2O_3 [13] and Eu/Eu* vs. Sm/Nd [9,11–13] show and confirm that the Campania bauxite values are very close to the Upper Continental Crust (UCC) average [32], which indicates materials of similar origin for all deposits, not related to a defined magmatic source nor to carbonate bed dissolution. During the Mesozoic, the Bahamian-type characteristics of the Apennine carbonate platform led to a rejection of the hypothesis that the source materials of the Campanian bauxite were transported to the platform via a hydrographic network, whereas it seems reasonable to state that the parent material was transported by wind [1,15,16,36].

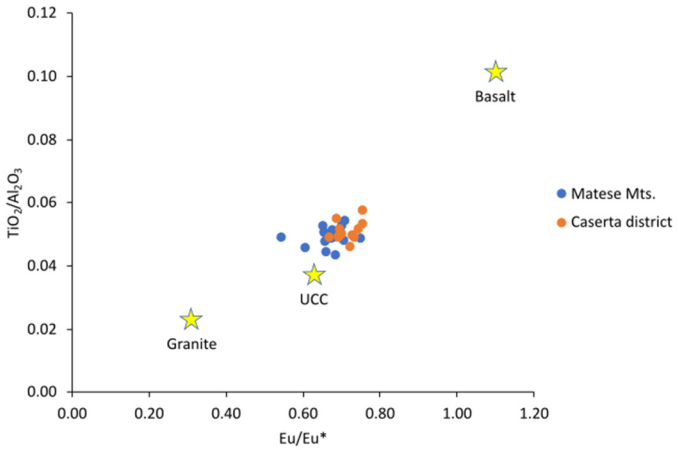

Figure 11. Eu/Eu* vs. TiO_2/Al_2O_3 binary diagram.

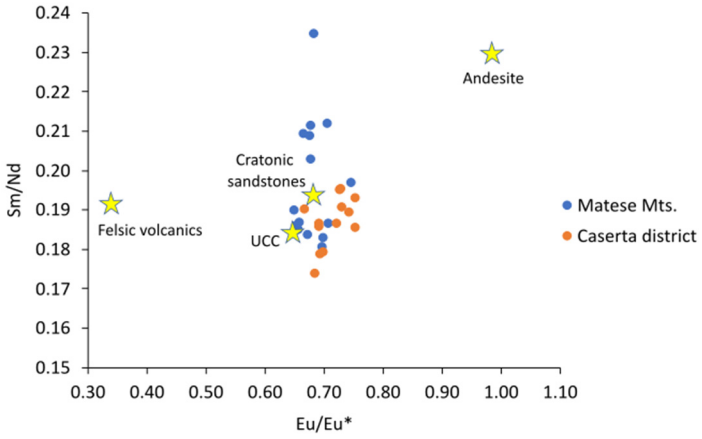

Figure 12. Eu/Eu* vs. Sm/Nd binary diagram. Felsic volcanic and cratonic sandstone values are from Condie [57]; UCC and andesite values are from Taylor and Mc Lennan [32].

6. Conclusions

1. The Campania region karst bauxite deposits, occurring in Matese Mts. and Caserta district, were classified as "bauxites" and "ferritic bauxites" and experienced strong laterization degrees.
2. Trace elements indicate that the bauxites in the Matese Mts. formed in a more aggressive and humid climate than the bauxites in the Caserta district, which are associated with a warmer climate and less aggressive climate conditions.
3. Weathering indices indicate high weathering degrees, reflecting a typical characteristic of residual deposits, such as bauxites, formed under intense climate conditions.
4. Paleo-precipitation indices showed that Matese Mts. bauxites experienced a more "humid" climate with respect to Caserta district bauxites.

5. Parental affinity binary diagrams confirmed eolian transport of bauxitic parent material, having an intermediate to mafic magmatic composition, evolving towards bauxite.

Author Contributions: Conceptualization, R.B.; methodology and analysis, R.B.; data curation, R.B.; writing—original draft preparation, R.B.; writing—review, and editing, G.M.; supervision, G.M. All authors have read and agreed to the published version of the manuscript.

Funding: This research received no external funding.

Data Availability Statement: Data sharing is not applicable to this article.

Conflicts of Interest: The authors declare no conflicts of interest.

References

1. Bardossy, G. *Karst Bauxites: Bauxite Deposits on Carbonate Rocks*; Elsevier: Amsterdam, The Netherlands, 1982.
2. D'Argenio, B.; Mindszenty, A. Bauxites and related paleokarst: Tectonic and climatic event markers at regional unconformities. *Eclogae Geol. Helv.* **1995**, *88*, 453–499.
3. Price, G.D.; Valdes, P.J.; Sellwood, B.W. Prediction of modern bauxite occurrence: Implications for climate reconstruction. *Palaeogeogr. Palaeoclimatol. Palaeoecol.* **1997**, *131*, 1–13. [CrossRef]
4. Bárdossy, G.; Combes, P.J. *Karst Bauxites: Interfingering of Deposition and Paleoweathering*; Blackwell Science: Oxford, UK, 1999; pp. 189–206.
5. Mongelli, G.; Buccione, R.; Sinisi, R. Genesis of autochthonous and allochthonous Apulian karst bauxites (Southern Italy): Climate constraints. *Sediment. Geol.* **2015**, *325*, 168–176. [CrossRef]
6. Mongelli, G.; Buccione, R.; Gueguen, E.; Langone, A.; Sinisi, R. Geochemistry of the Apulian allochthonous karst bauxite, Southern Italy: Distribution of critical elements and constraints on Late Cretaceous Peri-Tethyan palaeogeography. *Ore Geol. Rev.* **2016**, *77*, 246–259. [CrossRef]
7. Mongelli, G.; Boni, M.; Oggiano, G.; Mameli, P.; Sinisi, R.; Buccione, R.; Mondillo, N. Critical metals distribution in Tethyan karst bauxite: The Cretaceous Italian ores. *Ore Geol. Rev.* **2017**, *86*, 526–536. [CrossRef]
8. Mongelli, G.; Mameli, P.; Sinisi, R.; Buccione, R.; Oggiano, G. REEs and other critical raw materials in Cretaceous Mediterranean-type bauxite: The case of the Sardinian ore (Italy). *Ore Geol. Rev.* **2021**, *139*, 104559. [CrossRef]
9. Mongelli, G.; Boni, M.; Buccione, R.; Sinisi, R. Geochemistry of the Apulian karst bauxites southern Italy): Chemical fractionation and parental affinities. *Ore Geol. Rev.* **2014**, *63*, 9–21. [CrossRef]
10. Abedini, A.; Calagari, A.A. REE geochemical characteristics of titanium-rich bauxites: The Permian Kanigorgeh horizon, NW Iran. *Turk. J. Earth Sci.* **2014**, *23*, 513–532. [CrossRef]
11. Abedini, A.; Mongelli, G.; Khosravi, M. Geochemical constraints on the middle Triassic Kani Zarrineh karst bauxite deposit, Irano-Himalayan belt, NW Iran: Implications for elemental fractionation and parental affinity. *Ore Geol. Rev.* **2021**, *133*, 104099. [CrossRef]
12. Mameli, P.; Mongelli, G.; Sinisi, R.; Oggiano, G. Weathering Products of a Dismantled Variscan Basement. Minero-Chemical Proxies to Insight on Cretaceous Palaeogeography and Late Neogene Palaeoclimate of Sardinia (Italy). *Front. Earth Sci.* **2020**, *8*, 290. [CrossRef]
13. Yu, W.; Oggiano, G.; Mongelli, G.; Zhou, J.; Buccione, R.; Xu, L.; Mameli, P.; Du, Y. U-Pb detrital zircon ages and Hf isotope from Sardinia and Adria Cretaceous bauxite (Italy): Constraints on the Alpine Tethys paleogeography and tectonic evolution. *Ore Geol. Rev.* **2023**, *153*, 105272. [CrossRef]
14. Bogatyrev, B.A.; Zhukov, V.V. Bauxite provinces of the world. *Geol. Ore Depos.* **2009**, *51*, 339–355. [CrossRef]
15. Mondillo, N.; Balassone, G.; Boni, M.; Rollinson, G. Karst bauxites in the Campania Apennines (southern Italy): A new approach. *Period. Mineral.* **2011**, *80*, 407–432.
16. Boni, M.; Reddy, S.M.; Mondillo, N.; Balassone, G.; Taylor, R. A distant magmatic source for Cretaceous karst bauxites of Southern Apennines (Italy), revealed through SHRIMP zircon age dating. *Terra Nova* **2012**, *24*, 326–332. [CrossRef]
17. Buccione, R.; Mongelli, G.; Sinisi, R.; Boni, M. Relationship between geometric parameters and compositional data: A new approach to karst bauxites exploration. *J. Geochem. Explor.* **2016**, *169*, 192–201. [CrossRef]
18. Buccione, R.; Vitale, S.; Ciarcia, S.; Mongelli, G. Geochemistry and Geometrical Features of the Upper Cretaceous Vitulano Para-Autochthonous Karst Bauxites (Campania Region, Southern Italy): Constraints on Genesis and Deposition. *Minerals* **2023**, *13*, 386. [CrossRef]
19. Sinisi, R. Mineralogical and geochemical features of Cretaceous Bauxite from San Giovanni Rotondo (Apulia, Southern Italy): A provenance tool. *Minerals* **2018**, *8*, 567. [CrossRef]
20. Vitale, S.; Ciarcia, S. Tectono-stratigraphic setting of the Campania region (southern Italy). *J. Maps* **2018**, *14*, 9–21. [CrossRef]
21. Carannante, G.; Pugliese, A.; Ruberti, D.; Simone, L.; Vigliotti, M.; Vigorito, M. Evoluzione Cretacica di un settore della piattaforma apula da dati di sottosuolo e di affioramento (Appennino campano-molisano). *Ital. J. Geosci.* **2009**, *128*, 3–31.
22. Dewey, J.F.; Helman, M.L.; Knott, S.D.; Turco, E.; Hutton, D.H.W. Kinematics of the western Mediterranean. *Geol. Soc. Lond. Spec. Publ.* **1989**, *45*, 265–283. [CrossRef]

23. Channell, J.E.T.; D'Argenio, B.; Hovarth, F. Adria, the African promontory, in Mesozoic Mediterranean paleogeography. *Earth Sci. Rev.* **1979**, *15*, 213–292. [CrossRef]
24. Schettino, A.; Turco, E. Tectonic history of the western Tethys since the Late Triassic. *GSA Bull.* **2011**, *123*, 89–105. [CrossRef]
25. Carannante, G.; D'Argenio, B.; Mindszenty, A.; Ruberti, D.; Simone, L. Cretaceous-Miocene sequences. In *Regional Unconformities and Facies Patterns Field Trip Guidebook, 15th IAS Regional Meeting*; De Frede: Ischia, Italy, 1994; pp. 27–60.
26. Carannante, G.; D'Argenio, B.; Ferreri, V.; Simone, L. Cretaceous paleokarst of the Campanian Apennines from early diagenetic to late filling stage. A Case History. *Rend. Soc. Geol. Ital.* **1987**, *9*, 251–256.
27. D'Argenio, B.; Mindszenty, A.; Bárdossy, G.; Juhász, E.; Boni, M. Bauxites of Southern Italy revisited. *Rend. Soc. Geol. Ital.* **1986**, *9*, 263–268.
28. Bonardi, G.; Ciarcia, S.; Di Nocera, S.; Matano, F.; Sgrosso, I.; Torre, M. Carta delle principali unità cinematiche dell'Appennino meridionale. Nota illustrativa. *Ital. J. Geosci.* **2009**, *128*, 47–60.
29. Schellmann, W. A new definition of laterite. *Mem. Geol. Surv. India* **1986**, *120*, 1–7.
30. Aleva, G.J.J. Laterites: Concepts, Geology, Morphology and Chemistry. In *The Corlat Handbook*; Corlat Technical Publication; International Soil Reference and Information Center (ISRIC): Brussels, Belgium, 1994; pp. 8–21.
31. Boulange, B.; Ambrosi, J.P.; Nahon, D. Laterites and Bauxites. In *Soils and Sediments*; Springer: Berlin/Heidelberg, Germany, 1997.
32. Taylor, S.R.; McLennan, S.M. *The Continental Crust: Its Composition and Evolution*; Blackwell: Oxford, UK, 1985; pp. 1–312.
33. Davis, J.C. *Statistics and Data Analysis in Geology*; John Wiley & Sons: Hoboken, NJ, USA, 1986.
34. Bradl, H.B. Adsorption of heavy metal ions on soils and soils constituents. *J. Colloid Interface Sci.* **2004**, *277*, 1–18. [CrossRef]
35. Nesbitt, H.W. Mobility and fractionation of rare earth elements during weathering of a granodiorite. *Nature* **1979**, *279*, 206–210. [CrossRef]
36. Rieu, R.; Allen, P.A.; Plotze, M.; Pettke, T. Compositional and mineralogical variations in a Neoproterozoic glacially influenced succession, Mirbat area, south Oman: Implications for paleoweathering conditions. *Precambrian Res.* **2007**, *154*, 248–265. [CrossRef]
37. Yan, D.T.; Chen, D.Z.; Wang, Q.C.; Wang, J.G. Large–scale climatic fluctuations in the latest Ordovician on the Yangtze block, south China. *Geology* **2010**, *38*, 599–602. [CrossRef]
38. Suttner, L.J.; Dutta, P.K. Alluvial sandstones composition and paleoclimate; I, framework mineralogy. *J. Sediment. Petrol.* **1986**, *56*, 329–345.
39. Lerman, A. *The Lacustrine Chemistry Geology and Physics*; Geological Publishing House: Beijing, China, 1989.
40. Wang, W.X.; Fisher, N.S. Modeling the influence of body size on trace element accumulation in the mussel Mytilus edulis. *Mar. Ecol. Prog. Ser.* **1997**, *161*, 103–115. [CrossRef]
41. Perri, F.; Critelli, S.; Martín-Martín, M.; Montone, S.; Amendola, U. Unravelling hinterland and offshore palaeogeography from pre-to-syn-orogenic clastic sequences of the Betic Cordillera (Sierra Espuña), Spain. *Palaeogeogr. Palaeoclimatol. Palaeoecol.* **2017**, *468*, 52–69. [CrossRef]
42. Perri, F. Chemical weathering of crystalline rocks in contrasting climatic conditions using geochemical proxies: An overview. *Palaeogeogr. Palaeoclimatol. Palaeoecol.* **2020**, *556*, 109873. [CrossRef]
43. Nesbitt, H.W.; Young, G.M. Early Proterozoic climates and plate motions inferred from major element chemistry of lutites. *Nature* **1982**, *299*, 715–717. [CrossRef]
44. Michel, L.A.; Sheldon, N.D.; Myers, T.S.; Tabor, N.J. Assessment of pretreatment methods on CIA-K and CALMAG indices and the effects on paleoprecipitation estimates. *Palaeogeogr. Palaeoclimatol. Palaeoecol.* **2022**, *601*, 111102. [CrossRef]
45. Maynard, J.B. Chemistry of modern soils as a guide to interpreting Precambrian paleosols. *J. Geol.* **1992**, *100*, 279–289. [CrossRef]
46. Lukens, W.E.; Stinchcomb, L.C.; Nordt, D.J.; Kahle, S.G.; Driese, J.D. Tubbs Recursive Partitioning Improves Paleosol Proxies for Rainfall. *Am. J. Sci.* **2019**, *319*, 819–845.
47. Brimhall, G.H.; Lewis, C.J.; Ague, J.J.; Dietrich, W.E.; Hampel, J.; Rix, P. Metal enrichment in bauxites by deposition of chemically mature aeolian dust. *Nature* **1988**, *333*, 819–824. [CrossRef]
48. MacLean, W.H.; Bonavia, F.F.; Sanna, G. Argillite debris converted to bauxite during karst weathering: Evidence from immobile element geochemistry at the Olmedo De posit, Sardinia. *Miner. Depos.* **1997**, *32*, 607–616. [CrossRef]
49. Zamanian, H.; Ahmadnejad, F.; Zarasvandi, A. Mineralogical and geochemical investigations of the Mombi bauxite deposit, Zagros Mountains. *Iran. Geochem.* **2016**, *76*, 13–37. [CrossRef]
50. Lyew-Ayee, P.A. A case for the volcanic origin of Jamaican bauxites. Proceedings of the VI Bauxite Symposium 1986. *J. Geol. Soc.* **1986**, *1*, 9–39.
51. Morelli, F.; Cullers, R.; Laviano, R.; Mongelli, G. Geochemistry and paleoenvironmental significance of Upper Cretaceous clay-rich beds from the Peri-Adriatic Apulia carbonate platform, southern Italy. *Period. Mineral.* **2000**, *69*, 165–183.
52. Boni, M.; Rollinson, G.; Mondillo, N.; Balassone, G.; Santoro, L. Quantitative mineralogical characterization of karst bauxite deposits in the Southern Apennines, Italy. *Econ. Geol.* **2013**, *108*, 813–833. [CrossRef]
53. Esmaeily, D.; Rahimpour-Bonab, H.; Esna-Ashari, A.; Kananian, A. Petrography and geochemistry of the Jajarm Karst bauxite ore deposit, NE Iran: Implications for source rock material and ore genesis. *Turk. J. Earth Sci.* **2010**, *19*, 267–284.
54. Viers, J.; Wasserburg, G.J. Behavior of Sm and Nd in a lateritic soil profile. *Geochim. Cosmochim. Acta* **2004**, *68*, 2043–2054. [CrossRef]

55. Sinisi, R.; Mongelli, G.; Mameli, P.; Oggiano, G. Did the Variscan relief influence the Permian climate of Mesoeurope? Insights from geochemical and mineralogical proxies from Sardinia (Italy). *Palaeogeogr. Palaeoclimatol. Palaeoecol.* **2014**, *396*, 132–154. [CrossRef]
56. Gu, J.; Huang, Z.; Fan, H.; Jin, Z.; Yan, Z.; Zhang, J. Mineralogy, geochemistry, and genesis of lateritic bauxite deposits in the Wuchuan–Zheng'an–Daozhen area, Northern Guizhou Province, China. *J. Geochem. Explor.* **2013**, *130*, 44–59. [CrossRef]
57. Condie, K.C. Chemical composition and evolution of the upper continental crust: Contrasting results from surface samples and shales. *Chem. Geol.* **1993**, *104*, 1–37. [CrossRef]